

Formation of protonium in collisions of antiprotons with H and H⁻

James S. Cohen

Theoretical Division, Los Alamos National Laboratory, University of California, Los Alamos, New Mexico 87545

(Received 13 April 1987)

Cross sections for formation of protonium ($p\bar{p}$) in low-energy collisions of antiprotons with hydrogen atoms (H) and negative hydrogen ions (H⁻) are calculated using the classical-trajectory Monte Carlo (CTMC) method. Full four-body dynamics is performed for $\bar{p} + H^-$. Previously unpredicted differences between $\bar{p} + H$ and $\bar{p} + H^-$ collisions, stemming from the dynamics of the weakly bound electron in H⁻, are exhibited. A maximum protonium formation cross section of nearly 2 \AA^2 for $\bar{p} + H^-$ is found, smaller than previous theoretical estimates, but the reaction window is found to extend to higher energies. The electron stripping cross section for $\bar{p} + H^-$ collisions is also calculated and yields results in agreement with our previous three-body CTMC calculation and with a very recent experimental determination. The implications of these results for experiments with corotating beams of \bar{p} and H⁻ are discussed.

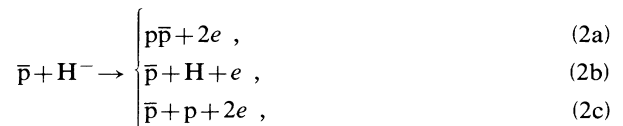
I. INTRODUCTION

The protonium atom ($p\bar{p}$) is of interest for research in atomic, nuclear, and particle physics. Studies of protonium represent an important part of the experimental program at the CERN low-energy antiproton ring (LEAR),¹⁻³ which has been in operation since 1983. The traditional way of forming $p\bar{p}$ is by stopping antiprotons in high-density hydrogen. The atoms are formed very efficiently in highly excited states, but because of large l mixing (Stark) rates in the dense fluid rather quickly reach an s , p , or d state and annihilate. New methods are now being developed for future experiments at LEAR. In one, a cyclotron trap will be used.^{1(c),1(d)} In another, corotating beams of antiprotons and negative hydrogen ions (H⁻) will be merged to form protonium in flight. These schemes offer the advantages of formation in isolation and high-resolution spectroscopy. A critical parameter in determining the practicality of the negative-ion technique is the ratio $\sigma_{p\bar{p}}/\sigma_{st}$ of the formation cross section to the stripping cross section. Stripping can occur either by intrabeam (H⁻ + H⁻) or interbeam ($\bar{p} + H^-$) interactions. The above ratio is important in the determination of the optimum \bar{p} and H⁻ beam intensities. A preliminary experiment at LEAR with a stored H⁻ beam demonstrated the influence of intrabeam stripping, but no quantitative experimental estimate was yet possible.^{3(b)} A fairly accurate theoretical calculation of stripping in $\bar{p} + H^-$ collisions has recently been published⁴ and indicates that the stripping cross section is somewhat smaller than previously calculated.⁵ A very recent experiment⁶ has determined the stripping cross section and corroborates the more recent theoretical calculation. In the present work, $p\bar{p}$ formation cross sections for $\bar{p} + H$ and $\bar{p} + H^-$ collisions are determined. The same $\bar{p} + H^-$ calculation also produces new estimates of the stripping cross section (because much larger impact parameters contribute to stripping than to $p\bar{p}$ formation, this was done for only three collision energies).

The reaction



occurs mainly at collision energies on the order of or less than the ionization potential of the target. The calculation of this cross section is done by the three-body classical-trajectory Monte Carlo (CTMC) method. The method is the same as previously used for negative muon (μ^-) capture by H.⁷ Those cross sections for μ^- are in good agreement with the limited experimental information available; the method should be even better for \bar{p} because capture occurs in still higher principal quantum-number states. For the reactions



a four-body CTMC calculation is made. Unlike reaction (1), all the pure Coulomb interactions cannot be used because classically the H⁻ would then generally autoionize. The potential used is described in Sec. II. The four-body trajectory method is described in Sec. III.

There are some noteworthy differences as well as similarities between reactions (1) and (2a). The total binding energy of H⁻ is slightly greater than that of H (the second electron is bound by 0.754 eV), and the H⁻ ion is much larger than the H atom, suggesting a larger cross section for (2a). However, in a previous calculation based on the adiabatic ionization model, the cross sections for H and H⁻ were predicted to differ negligibly at $E \gtrsim 0.1$ a.u.⁸ An important difference between $\bar{p} + H$ and $\bar{p} + H^-$ is the Coulomb repulsion with the negative ion. In the former reaction, the relative potential energy is purely attractive and the $p\bar{p}$ -formation cross section increases monotonically as the collision energy decreases. In the latter reaction, however, the two negative species are unable to approach closely at very low energies so the cross section goes to zero. This implies that $p\bar{p}$ formation appreciably occurs in only a rather narrow energy "window." Bracci *et al.*⁸ found this window to span $0.03 \lesssim E \leq 0.5$ a.u.; intriguingly, their cross section appeared to peak sharply at very low energy ($E \simeq 0.05$ a.u.) where stripping^{4,5} is impro-

able. The CTMC cross sections for (1) and (2) are presented in Sec. IV. The cross-section window is found to be shifted to higher energies and leveled with respect to Ref. 8. The *dynamic* effects of electrostatic repulsion at low energy and of kinetic energy transferred to the weakly bound electron at higher energy are shown to be important.

II. POTENTIAL ENERGY FOR $\bar{p} + \text{H}^-$

In reality, the complete potential for $\bar{p} + \text{H}^-$ is just the sum of the Coulomb potentials between \bar{p} , p , and two electrons. However, a classical H^- ion is not stable (it usually autoionizes in less than a collision time at the energies of interest), so judicious use of quantum-mechanical information is called for.⁹ In Ref. 4 the neutral H atom was treated as a polarizable core, and the second electron was bound by an effective core-plus-polarization potential, a *two*-body potential. Though exactly that treatment does not suffice for the target in $\bar{p}\bar{p}$ formation, a slight variation does. In the present work, H^- is described by a *three*-body potential, but correlation between the two electrons is neglected. The first electron is subject to the full nuclear charge, whereas the second electron is subject only to the time-averaged combined effect of the nucleus and first electron as in Ref. 4. This is realistic because the core electron responds adiabatically to perturbations by the weakly bound electron. On the other hand, the \bar{p} projectile interacts with all three particles in the target with pure Coulomb potentials. The resulting potential, in terms of the distances defined in Fig. 1, is (in atomic units)

$$V_{\text{tot}} = -\frac{1}{R_1} + \frac{1}{R_3} + \frac{1}{R_4} - \frac{1}{R_2} - V_{\text{core}}(R_6) + V_{\text{pol}}(R_6), \quad (3)$$

where

$$V_{\text{core}}(r) = \left[\frac{1}{r} + 1 \right] e^{-2r} \quad (4)$$

and

$$V_{\text{pol}}(r) = -\frac{\alpha_{\text{H}}}{2r^4} \exp(-r_0^2/r^2), \quad (5)$$

with $\alpha_{\text{H}} = 4.5$ a.u. and $r_0 = 1.596a_0$.⁴ The potential given by the last two terms of Eq. (3) *quantum mechanically*

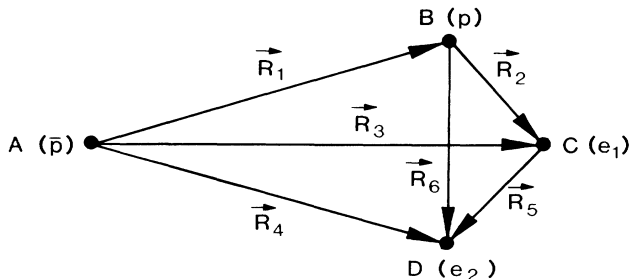


FIG. 1. Interparticle coordinates.

binds an electron by the actual electron affinity of the H atom.

Note that Eq. (3) does not contain R_5 so there is no direct interaction between the two electrons. However, autoionization of this classical H^- atom still occurs eventually because of the indirect energy transfer mediated by the nucleus. The time for autoionization is long enough that it might nevertheless be possible to describe the target in this way. However, an additional minor modification makes the classical H^- ion stable for all time; namely, the nucleus is given infinite mass. To ensure that this alteration has minimal effect on the collision dynamics, the masses of the other particles are also changed so that the e - p and p - \bar{p} reduced masses are correct. The only error made is a slightly small e - \bar{p} mass, but this deviation is quite negligible.

III. CTMC METHOD

The calculations were done with an expanded version of the program used⁷ for $\mu^- + \text{H}$ and immediately applicable to $\bar{p} + \text{H}$. The colliding particles were previously designated $A + BC$, so for consistency the extra electron of H^- is designated D . For efficiency, the calculations are done in the center-of-mass (c.m.) system; the required transformations between different c.m. systems are described below. A rudimentary version of this program was used to treat the $d\mu + de$ collision,¹⁰ and the coordinate system for solution of Hamilton's equations was already selected for that problem.

A. Hamilton's equations

The Hamiltonian in the $AD + BC$ c.m. coordinate system, illustrated in Fig. 2(a), is

$$H = (2\mu_{BC})^{-1} | \mathbf{P}_1 |^2 + (2\mu_{AD,BC})^{-1} | \mathbf{P}_2 |^2 + (2\mu_{AD})^{-1} | \mathbf{P}_3 |^2 + V(\mathbf{Q}_1, \mathbf{Q}_2, \mathbf{Q}_3), \quad (6)$$

where the notation

$$\mu_{ij}^{-1} = m_i^{-1} + m_j^{-1}, \quad (7a)$$

and

$$\mu_{ij,kl}^{-1} = (m_i + m_j)^{-1} + (m_k + m_l)^{-1} \quad (7b)$$

is used for the various reduced masses required. Hamilton's equations of motion are then obtained by

$$\dot{Q}_{ji} = \frac{\partial H}{\partial P_{ji}} \quad (8a)$$

and

$$-\dot{P}_{ji} = \frac{\partial H}{\partial Q_{ji}}. \quad (8b)$$

Because the potential V in Eq. (3) is expressed in terms of the interparticle distances, a more convenient form is attained by applying the chain rule to rewrite Eq. (8b) as

$$-\dot{P}_{ji} = \sum_{k=1}^6 \frac{R_{ki}}{R_k} \frac{\partial R_{ki}}{\partial Q_{ji}} \frac{\partial V}{\partial R_k}. \quad (9)$$

The partial derivatives of the components of the internu-

clear vectors with respect to the $AD + BC$ frame coordinates are the elements of the transformation matrix in

$$\begin{pmatrix} \mathbf{R}_1 \\ \mathbf{R}_2 \\ \mathbf{R}_3 \\ \mathbf{R}_4 \\ \mathbf{R}_5 \\ \mathbf{R}_6 \end{pmatrix} = \begin{pmatrix} -\alpha_2 & -1 & \alpha_4 \\ 1 & 0 & 0 \\ 1 - \alpha_2 & -1 & \alpha_4 \\ 0 & 0 & 1 \\ -1 + \alpha_2 & 1 & 1 - \alpha_4 \\ \alpha_2 & 1 & 1 - \alpha_4 \end{pmatrix} \begin{pmatrix} \mathbf{Q}_1 \\ \mathbf{Q}_2 \\ \mathbf{Q}_3 \end{pmatrix}, \quad (10)$$

where $\alpha_2 = m_C / (m_B + m_C)$ and $\alpha_4 = m_D / (m_A + m_D)$. For later use, we also give here the transformation to the *relative* momenta between pairs of particles,

$$\begin{pmatrix} \mathbf{P}_1^{\text{rel}} \\ \mathbf{P}_2^{\text{rel}} \\ \mathbf{P}_3^{\text{rel}} \\ \mathbf{P}_4^{\text{rel}} \\ \mathbf{P}_5^{\text{rel}} \\ \mathbf{P}_6^{\text{rel}} \end{pmatrix} = \begin{pmatrix} -\alpha_1 & -\mu_{AB} / \mu_{AD,BC} & 1 - \alpha_1 \\ 1 & 0 & 0 \\ 1 - \alpha_3 & -\mu_{AC} / \mu_{AD,BC} & \alpha_3 \\ 0 & 0 & 1 \\ -\alpha_5 & \mu_{CD} / \mu_{AD,BC} & 1 - \alpha_5 \\ \alpha_6 & \mu_{BD} / \mu_{AD,BC} & 1 - \alpha_6 \end{pmatrix} \begin{pmatrix} \mathbf{P}_1 \\ \mathbf{P}_2 \\ \mathbf{P}_3 \end{pmatrix}, \quad (11)$$

where $\alpha_1 = m_A / (m_A + m_B)$, $\alpha_3 = m_C / (m_A + m_C)$, $\alpha_5 = m_D / (m_C + m_D)$, and $\alpha_6 = m_D / (m_B + m_D)$.

The system of equations (8) was numerically integrated using the sixth-order Gear hybrid method.¹¹ All derivatives were evaluated analytically.

B. Transformations between coordinate systems

Though the equations of motion are solved in the $AD + BC$ coordinate system of Fig. 2(a), the initial and final states of the present problem are most naturally described in the $A + BCD$ coordinate system, designated \mathbf{Q}_j^0 , and the $AB + CD$ coordinates system, designated \mathbf{Q}_j' , illustrated in Figs. 2(b) and 2(c), respectively. The c.m. motion is separated in all these systems and can be ignored here. The initial coordinates and momenta (see Sec. III C) are transformed to appropriate initial conditions for the equations specified in Sec. III A by¹²

$$\underline{\mathbf{Q}} = \underline{\mathbf{C}} \underline{\mathbf{Q}}^0 \quad (12a)$$

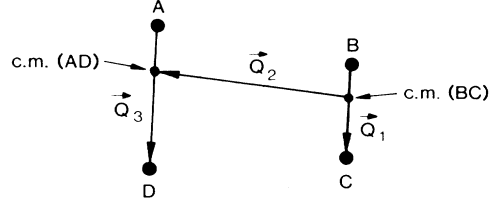
and

$$\underline{\mathbf{P}} = \underline{\mathbf{C}}^{-1} \underline{\mathbf{P}}^0, \quad (12b) \quad \text{and}$$

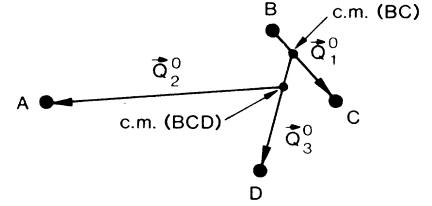
$$\underline{\mathbf{C}}^{-1} = \begin{pmatrix} 1 & 0 & 0 \\ 0 & \frac{m_B + m_C}{m_B + m_C + m_D} & -\frac{m_D(m_A + m_B + m_C + m_D)}{(m_A + m_D)(m_B + m_C + m_D)} \\ 0 & 1 & \frac{m_A}{m_A + m_D} \end{pmatrix}. \quad (13b)$$

[Note that the transpose of Eq. (13b) appears in Eq. (12b).] If no rearrangement occurs in the collision (i.e., if $p\bar{p}$ is not formed), then the $A + BCD$ coordinate system is once again appropriate and the solution is transformed

(a)



(b)



(c)

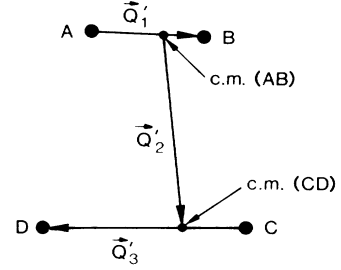


FIG. 2. Barycentric coordinate systems used in the present work: (a) $AD + BC$ system, (b) $A + BCD$ system, (c) $AB + CD$ system.

where

$$\underline{\mathbf{C}} = \begin{pmatrix} 1 & 0 & 0 \\ 0 & \frac{m_A}{m_A + m_D} & \frac{m_D(m_A + m_B + m_C + m_D)}{(m_A + m_D)(m_B + m_C + m_D)} \\ 0 & -1 & \frac{m_B + m_C}{m_B + m_C + m_D} \end{pmatrix} \quad (13a)$$

back to it by

$$\underline{\mathbf{Q}}^0 = \underline{\mathbf{C}}^{-1} \underline{\mathbf{Q}} \quad (14a)$$

and

$$\mathbf{P}^0 = \bar{\mathbf{C}} \mathbf{P} . \quad (14b)$$

If $p\bar{p}$ is formed, then the $AB + CD$ coordinate system of Fig. 2(c) is appropriate and the solutions are taken into this system by

$$\mathbf{Q}' = \underline{\mathbf{B}}^{-1} \mathbf{Q} \quad (15a)$$

and

$$\mathbf{P}' = \underline{\mathbf{B}} \mathbf{P} , \quad (15b)$$

where

$$\underline{\mathbf{B}} = \begin{pmatrix} -\frac{m_A}{m_A + m_B} & 1 & -\frac{m_D}{m_C + m_D} \\ -\frac{\mu_{AB}}{\mu_{AD,BC}} & \frac{m_B m_D - m_A m_C}{(m_A + m_D)(m_B + m_C)} & \frac{\mu_{CD}}{\mu_{AD,BC}} \\ \frac{m_B}{m_A + m_B} & 1 & \frac{m_C}{m_C + m_D} \end{pmatrix} \quad (16a)$$

and

$$\underline{\mathbf{B}}^{-1} = \begin{pmatrix} -\frac{m_C}{m_B + m_C} & -1 & \frac{m_D}{m_A + m_D} \\ \frac{\mu_{BC}}{\mu_{AB,CD}} & \frac{m_B m_D - m_A m_C}{(m_A + m_B)(m_C + m_D)} & \frac{\mu_{AD}}{\mu_{AB,CD}} \\ -\frac{m_B}{m_B + m_C} & 1 & \frac{m_A}{m_A + m_D} \end{pmatrix} . \quad (16b)$$

C. Initial conditions

The initial coordinates and momenta of the two electrons of H^- are sampled from microcanonical distributions, i.e., from on-the-energy-shell δ functions at energies -0.4997 and -0.0277 a.u. The values for the first electron, which is subject to a pure Coulomb potential, are easily generated directly from random numbers following a procedure previously described in detail.¹³ Simply stated, it corresponds to orbitals having uniform distribution of the angular momentum squared between 0 and 1, and having random orientation and random phase. For the second electron, facing a more complicated potential, the distribution is sampled by the numerical procedure described in Ref. 4. The numerical approximation to a δ function is taken to have a Gaussian width equal to 1% of the binding energy, so the actual binding energies fall in a narrow band of about ± 0.0003 a.u. The maximum distance and momentum sampled were 2.9 (the maximum classical turning point) and 3.0, respectively, in atomic units.

D. Final state

The trajectories were integrated until the final state could be clearly identified. For $p\bar{p}$ formation, passing of all the following tests was required:

- (1) $R_2, R_3, R_4, R_6 > R_s$,
- (2) $E_2^{\text{rel}}, E_6^{\text{rel}} > 0$,
- (3) $E_1^{\text{rel}} < 0$,
- (4) $\gamma |E_1^{\text{rel}}| > \frac{1}{R_3} + \frac{1}{R_4} + \frac{1}{R_2}$
 $+ | -V_{\text{core}}(R_6) + V_{\text{pol}}(R_6) |$,

where E_k^{rel} is the internal energy of the pair of particles corresponding to the interparticle distance R_k . The values $R_s = 4a_0$ and $\gamma = 0.2$ were used. By this point, the classically derived "quantum" numbers⁷ n and l of the capture orbital were also found to have reached their asymptotic values. Total energy and angular momentum were accurately conserved in all trajectories.

Though the runs done on $\bar{p} + \text{H}^-$ to obtain $\sigma_{p\bar{p}}$ also include stripping, much larger impact parameters are needed for the convergence of σ_{st} ; furthermore, stripping still occurs and is of interest at higher energies. Hence separate runs to obtain the stripping cross sections are expedient. The conditions required for stripping are

- (1) $R_1 > R_s$,
- (2) $E_1^{\text{rel}} > 0$,
- (3) $\mathbf{R}_1 \cdot \mathbf{P}_1^{\text{rel}} > 0$,
- (4a) $R_2 > R_s$ or (4b) $R_6 > R_s$,
- (5a) $\gamma E_2^{\text{rel}} > \frac{1}{R_1} + \frac{1}{R_3}$ or (5b) $\gamma E_6^{\text{rel}} > \frac{1}{R_1} + \frac{1}{R_4}$,

where a applies to the tightly bound electron and b applies to the weakly bound electron. As in Ref. 4, $R_s = 10a_0$ and $\gamma = 0.6$ were used. There are a few trajectories where (4b) cannot be satisfied but which are still reasonably counted as stripping of the weakly bound-electron. This situation occurs when such an electron becomes quasibound (at positive energy) by the centrifugal barrier formed with the polarization potential (such an effect is not possible with a Coulomb potential). Because such a state would decay quantum mechanically, the result is reasonably interpreted as stripping. Howev-

er, such trajectories are rare enough that the effect on the cross section is well within the stated statistical uncertainties.

IV. RESULTS AND DISCUSSION (REF. 14)

A. Protonium formation cross sections for $\bar{p} + H$ and $\bar{p} + H^-$

The calculated cross sections for $p\bar{p}$ formation in $\bar{p} + H$ and $\bar{p} + H^-$ collisions are given in Table I. We first observe that the cross sections for H and H^- are quite different from each other in *both* the low and the high ranges of the energy, their magnitudes crossing just above 0.5 a.u. The difference at low energy is obviously attributable to the Coulomb repulsion between \bar{p} and H^- , although, as discussed below, electrostatics apparently does not suffice to obtain the cutoff quantitatively. The difference at $E > 0.5$ a.u. might be considered somewhat more surprising in view of the small difference (0.0277 a.u.) in total binding energies of H and H^- . While the cross section for H falls steeply at $E > 0.5$ a.u., a similar drop in the H^- cross section does not occur until $E > 0.7$ a.u. Examination of the energies of the two electrons ionized from H^- yields a clue. The tightly bound electron usually carries away little kinetic energy, just as it does in $\bar{p} + H$ collisions. However, the weakly bound electron carries away considerably more kinetic energy. The explanation is simple. The electrons are uncorrelated and ejected sequentially. The weakly bound electron leaves first, (asymptotically) in the repulsive Coulomb field provided by the other three particles, and thereby gains kinetic energy. The other electron then escapes in a weak field similar to that occurring in $\bar{p} + H$ collisions. The balance of the above two effects results in an energy dependence of the $p\bar{p}$ formation cross section for $\bar{p} + H^-$ that displays a broad plateau in contrast to the energetically monotonic $\bar{p} + H$ cross section.

The present calculation of $\sigma_{p\bar{p}}(\bar{p} + H^-)$ is compared in Fig. 3 with that calculated by Bracci *et al.*⁸ using a model based on the adiabatic ionization concept. The present results find the peak cross section to be about a factor of 4 smaller and the low-end cutoff to occur at a rather higher energy. Apparently a static calculation

TABLE I. Protonium formation cross sections for $\bar{p} + H$ and $\bar{p} + H^-$.

E (a.u.)	$\sigma_{p\bar{p}}(10^{-16} \text{ cm}^2)^a$	
	$\bar{p} + H$	$\bar{p} + H^-$
0.05	6.92±0.26	
0.10	4.59±0.17	0.04±0.04
0.20	3.22±0.15	1.65±0.18
0.30	2.76±0.17	1.78±0.13
0.40	2.52±0.12	1.85±0.14
0.50	2.31±0.10	1.84±0.11
0.55	0.87±0.06	1.73±0.13
0.60	0.16±0.03	1.71±0.13
0.70	0.03±0.01	1.41±0.12
0.80		0.32±0.07
0.90		0.05±0.03

^aError estimates are statistical only (one standard deviation).

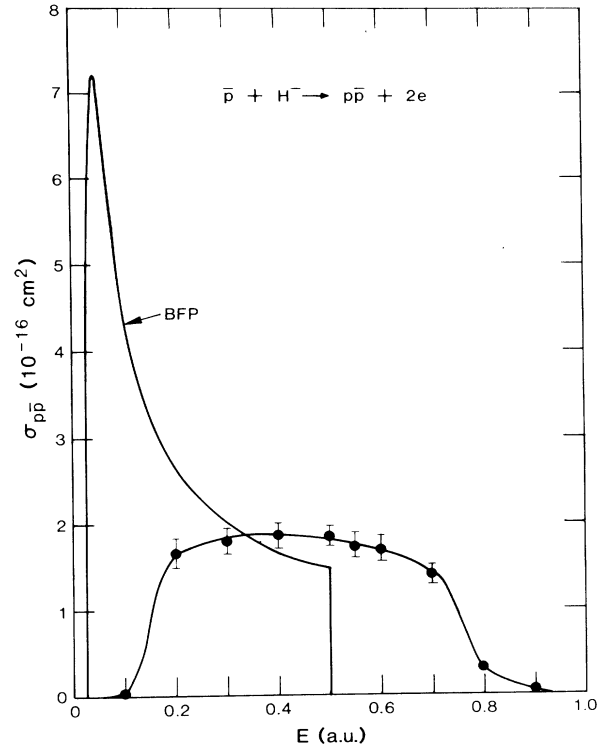


FIG. 3. Cross section for protonium formation in collisions of antiprotons with negative hydrogen ions. The earlier result of Bracci *et al.* (Ref. 8) is shown for comparison (labeled BFP). Note: 1 a.u. = 27.21 eV.

does not suffice. At the high end, the present cross section is much larger than that found by Bracci *et al.*, suggesting that the concept of adiabatic ionization needs to be modified for collisions of a negative particle with a negative ion. In such a case, the final-state field, ignored in the usual formulation of adiabatic ionization, must be taken into account. At present, no experimental cross sections for $p\bar{p}$ formation in $\bar{p} + H^-$ collisions are available.

The *average* n and l quantum numbers of the initially formed $p\bar{p}$ atoms are given in Table II. The states initially populated in capture by H and by H^- are similar. However, the subsequent cascades also depend greatly on the host targets, which are typically quite different for H

TABLE II. Average values of n and l quantum numbers of initially formed protonium atoms.

E (a.u.)	\bar{n}		\bar{l}	
	$\bar{p} + H$	$\bar{p} + H^-$	$\bar{p} + H$	$\bar{p} + H^-$
0.05	30.5		19.2	
0.10	32.2		21.1	
0.20	36.5	30.2	24.2	18.6
0.30	43.6	33.3	26.9	22.0
0.40	57.2	37.7	31.3	25.6
0.50	121	45.2	34.3	28.5
0.55	201	51.8	30.1	30.2
0.60	219	60.5	24.0	31.1
0.70		131		34.8
0.80		154		31.3

and H^- . In future work, we will characterize the n and l distributions and their effects on cascade x rays and annihilation states.

It is instructive to compare $\sigma_{p\bar{p}}(\bar{p} + H)$ with the cross section previously calculated for muonic hydrogen formation,⁷ $\sigma_{p\mu}(\mu^- + H)$. Figure 4 shows that these two cross sections are quite similar, differing significantly only at $E > 0.5$ a.u., where $\sigma_{p\bar{p}}$ cuts off more rapidly. This difference is expected because, at a given energy, the proton is slower and less capable of transferring energy to the target electron.

B. Stripping of H^- in collisions with \bar{p}

Four-body calculations for $\bar{p} + H^-$ collisions at velocities of 0.03, 0.10, and 1.0 a.u. were extended to large impact parameters in order to converge the stripping cross sections [reactions (2b) and (2c)]. The resulting cross sections are given in Table III where they are also compared with the three-body results from Ref. 4. The agreement with the previous calculations is within statistical errors and confirms the validity of the polarizable H core potential used in that work. Note that the four-body calculations take much more computation than the corresponding three-body calculations; this is not due to the extra equations (a 50% increase) as much as it is due to the smaller time step required to describe the rapid motion of the tightly bound electron. The experimental

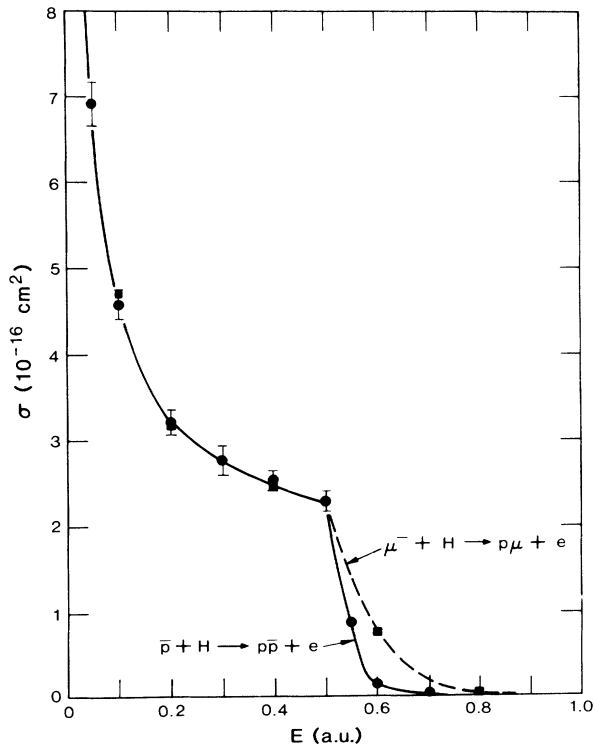


FIG. 4. Cross section for protonium formation (circles) in collisions of antiprotons with hydrogen atoms. The cross section for muonic hydrogen formation (squares), shown for comparison, is essentially the same below 0.5 a.u. The energy is for the c.m. system (as it is throughout this paper).

TABLE III. Cross sections for stripping of H^- in collisions with \bar{p} .

E (a.u.)	v_{rel} (ac)	σ_{st} (10^{-16} cm 2)	
		Present	Ref. 4
0.413	0.03	32.4 ± 3.2	33.2 ± 2.8
4.593	0.1	36.5 ± 2.6	37.7 ± 3.8
459.3	1.0	22.2 ± 1.7	19.1 ± 2.1

value⁶ of $36 \pm 1 \text{ \AA}^2$, obtained very recently for stripping in $H^- + H^-$ collisions at $v \approx 0.05$ a.u., also is in agreement with our theoretical values.

The four-body calculations enable us to discern the relative contributions of double-electron (2c) and single-electron (2b) stripping. Of course, at collision energies less than 14.4 eV ($v = 0.034$ a.u.), only single-electron removal is energetically possible without attendant $p\bar{p}$ formation. In the calculations at $v = 0.1$, no double-electron stripping was yet found. At $v = 1.0$, both electrons were removed in about 9% of the stripping reactions. In no case was the tightly bound electron stripped without the weakly bound electron (classically distinguishable) also being stripped; this observation tends to verify the assumption that electron-electron correlation can be neglected.

V. CONCLUSIONS

The competitive stripping and protonium-formation cross sections for $\bar{p} + H^-$ collisions are exhibited together in Fig. 5. The present and recent CTMC calculations⁴

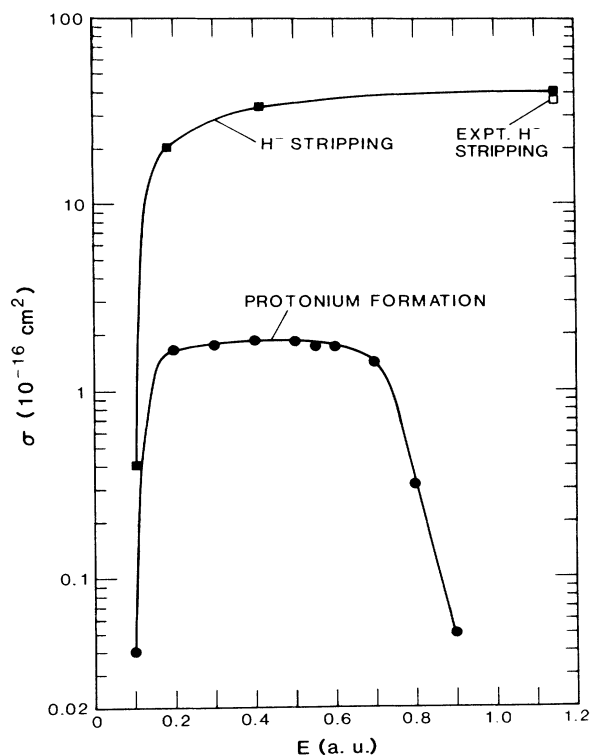


FIG. 5. Stripping cross section (from Ref. 4) and protonium-formation cross section for $\bar{p} + H^-$ collisions. The experimental point is from Chanel *et al.* (Ref. 6), obtained in $H^- + H^-$ collisions.

and the very recent experimental measurement⁶ yield H^- stripping cross sections smaller than earlier estimates,⁵ thereby permitting greater beam intensities. This advantage is partly offset by the current finding that the maximum protonium formation cross section for $\bar{p} + H^-$ is also smaller than previously calculated,⁸ by about the same factor. However, the new maximum occurs at a higher energy and the cross section is rather flat between 5 and 20 eV. Hence the requirement on the acceptable beam momentum spread is not so stringent. Because the present calculations show that protonium formation is very slow below 3 eV, where it was previously predicted to peak,⁸ less cooling may be desirable than formerly thought. One effect of this shift is to close the window where the protonium cross section once appeared to be

larger than the stripping cross section.^{5,8}

The protonium atoms are formed with quite high principal quantum numbers n and usually high angular momentum l . Formation under conditions suppressing collisional l mixing should allow long lifetimes and low- n states to be reached before annihilation. Such conditions may be achievable in a low-density gas utilizing a cyclotron trap, or with the technique of merged corotating \bar{p} and H^- beams.

ACKNOWLEDGMENTS

The author thanks Professor G. Fiorentini for suggesting this problem. This work was performed under the auspices of the U.S. Department of Energy.

¹(a) J. M. Richard in *Physics at LEAR with Low-Energy Cooled Antiprotons*, Proceedings of the Workshop on Physics at LEAR on Low-Energy Cooled Antiprotons, Erice, 1982, edited by U. Gastaldi and R. Klapisch (Plenum, New York, 1984), p. 83; (b) U. Gastaldi and D. Möhl *ibid.*, p. 649; (c) L. M. Simons *ibid.*, p. 155; (d) D. Gotta *ibid.*, p. 165; and others.

²*Antiproton 1984*, Proceedings of the Seventh European Symposium on Antiproton Interactions, Durham, 1984, edited by M. R. Pennington (Adam Hilger, Bristol, 1985), Sec. 3.

³(a) D. Möhl, in *Physics with Antiprotons at LEAR in the ACOL Era*, Proceedings of the Third LEAR Workshop, Tignes, 1985, edited by U. Gastaldi, R. Klapisch, J. M. Richard, and J. Tran Thanh Van (Frontières, Gif sur Yvette, France, 1985), p. 65; (b) E. Asseo *et al.*, *ibid.*, p. 99; and others.

⁴J. S. Cohen and G. Fiorentini, *Phys. Rev. A* **33**, 1590 (1986).

⁵G. Fiorentini and R. Tripiccione, *Phys. Rev. A* **27**, 737 (1983).

⁶M. Chanel *et al.*, CERN Report No. PS 87-12 (LEA), 1987 (unpublished).

⁷J. S. Cohen, *Phys. Rev. A* **27**, 167 (1983).

⁸L. Bracci, G. Fiorentini, and O. Pitzurra, *Phys. Lett.* **85B**, 280 (1979).

⁹Quasistable classical orbitals are not useful as they may autoionize even when very weakly perturbed. In addition, they do not properly sample the relevant phase space.

¹⁰J. S. Cohen, *Phys. Rev. A* **35**, 1419 (1987).

¹¹C. W. Gear, Illinois Computation Center Technical Report No. 164, 1964 (unpublished).

¹²L. M. Raff, D. L. Thompson, L. B. Sims, and R. N. Porter, *J. Chem. Phys.* **56**, 5998 (1972). The transformation $Q^0 \rightarrow Q$ is given in this reference, but the equations corresponding to Eqs. (12b) and (13b) appear to be in error.

¹³J. S. Cohen, *Phys. Rev. A* **26**, 3008 (1982).

¹⁴Atomic units ($\hbar = e = m_e = 1$) are used except where otherwise stated. Corresponding units used are energy 1 a.u. = 27.21 eV, distance 1 $a_0 = 5.292 \times 10^{-9}$ cm, cross section 1 $a_0^2 = 2.800 \times 10^{-17}$ cm², and velocity 1 a.u. = $ac = 2.188 \times 10^8$ cm/s.